Biomaterials 255 (2020) 120176

Contents lists available at ScienceDirect

Biomaterials

journal homepage: www.elsevier.com/locate/biomaterials

Bio-orthogonally crosslinked hyaluronate-collagen hydrogel for suture-free corneal defect repair

Fang Chen[a,b], Peter Le[a,b], Gabriella M. Fernandes-Cunha[a], Sarah C. Heilshorn[c], David Myung[a,b,d,*]

[a] Ophthalmology, Stanford University School of Medicine, CA, United States
[b] VA Palo Alto Health Care System, Palo Alto, CA, United States
[c] Materials Science & Engineering, Stanford University, CA, United States
[d] Chemical Engineering, Stanford University, CA, United States

ARTICLE INFO

Keywords:
Hyaluronate-collagen hydrogel
Bio-orthogonal
SPAAC crosslinking
Corneal wound repair
Sutureless repair
Cornea substitute

ABSTRACT

Biomaterials that mimic corneal stroma could decrease the need for donor corneal tissue and could decrease the prevalence of complications associated with corneal transplantation, including infection and rejection. We developed a bio-orthogonally crosslinked hyaluronate-collagen hydrogel which can fill corneal defects in situ without the need for any sutures, initiators, or catalysts. We studied the effects of biorthogonal crosslinking on the light transmittance of the hydrogel, which was greater than 97% water. The transmittance of the optimized hydrogel in the visible light range was over 94%. We also investigated the mechanical properties, refractive index, morphology, biocompatibility, and corneal re-epithelialization capacity of the hyaluronate-collagen hydrogel. Our *in vitro, in vivo,* and *ex vivo* results demonstrated that this bio-orthogonally crosslinked hyaluronate-collagen hydrogel has excellent potential as a biomaterial for cornea repair and regeneration.

1. Introduction

The cornea is the dome-shaped and transparent outermost part of the eye. It serves a critical dual role in both focusing light onto and providing protection for intraocular neurosensory structures. Corneal injury or diseases can quickly lead to scarring and thinning of the cornea, eventually leading to blindness, which has been estimated to affect 23 million people worldwide [1]. Although corneal transplantation can treat corneal blindness effectively, it benefits less than 1.5% of patients with corneal blindness due to the shortage of donor corneas and a global imbalance in donor cornea supply and demand [2]. Moreover, although corneas are immune-privileged compared to most tissues in the body, a transplanted donor cornea is still at risk of serious complications such as infection and rejection [3]. Traditional cornea transplantation, penetrating keratoplasty (PKP), also has the inherent risk of graft dehiscence, i.e. wound separation, with even minor trauma. Although some of these risks can be addressed by novel corneal transplantation techniques, such as Deep Anterior Lamellar Keratoplasty (DALK), these advanced procedures are not available for most cases worldwide [2]. Endothelial keratoplasty has emerged as a sutureless way to replace just the endothelium of corneas in cases of Fuch's dystrophy or other causes of bullous keratopathy [4]. However, surgical treatment of any damage or scarring anterior to the endothelium requires meticulous dissection, precise sizing, and numerous sutures for proper placement as a full thickness or anterior lamellar graft.

A promising strategy to overcome these limitations of corneal transplantation is using biomaterials to replace damaged corneal tissue. Currently, cyanoacrylate glue is used off-label clinically as a temporizing agent to stabilize corneal defects prior to corneal transplantation, but it forms an opaque plaque that offers no improvement in vision. Typical biomaterials being developed for corneal tissue engineering are hydrogels, which are networks of hydrophilic polymer chains that can hold a large amount of water. An ideal hydrogel for cornea replacement should have similar physical, chemical, and biological properties to those of native corneal stromal tissue. The fundamental features of an ideal hydrogel that mimics native cornea include: 1) high transparency for visible light transmittance, 2) high water content, 3) mechanical stability on the cornea after application, 4) no toxicity nor toxic decomposition products, 5) good biointegration but no interference with adjacent tissues, 6) suppor for the physiobiological functions of adjacent tissues, and 7) ease of application [5]. These features are heavily dependent on both the nature of the polymers and the crosslinking method involved.

An in situ-forming hydrogel that can be applied to a corneal defect to form a stromal tissue substitute could attend to these requirements without the need for sutures or even incisions. In this work, we describe

* Corresponding author. Ophthalmology, Stanford University School of Medicine, CA, United States.
E-mail address: david.myung@stanford.edu (D. Myung).

https://doi.org/10.1016/j.biomaterials.2020.120176
Received 10 February 2020; Received in revised form 28 May 2020; Accepted 4 June 2020
Available online 10 June 2020
0142-9612/ Published by Elsevier Ltd.

a novel hydrogel that flows into corneal defects and crosslinks within minutes to form a solid gel. The hydrogel is composed of collagen and hyaluronate, both of which are naturally derived polymers. Collagen is the main component of native corneal stromal tissue [6]. A crosslinked recombinant human collagen type III-based implant (RHCIII-MPC) has been reported to improve the vision of patients with scarred or ulcerated corneas from severe infection [1]. Sani et al. have developed a bio-adhesive hydrogel for sutureless repair of corneal wounds based on gelatin (a derivative of collagen) photo-crosslinked with visible light [7]. This hydrogel showed comparable physical properties to cornea and promoted stromal regeneration and re-epithelization. Li et al. also reported on a gelatin-based, photochemically cured gel with similar results [8]. Previously, our lab developed a collagen-based hydrogel which could bio-orthogonally crosslink and form in situ [9]. This collagen gel could encapsulate keratocytes and support the growth of corneal epithelial cells. Hyaluronate is a sodium salt of hyaluronic acid (HA), which is a naturally mucoadhesive polysaccharide commonly existing in human connective tissues. HA has been reported to promote corneal epithelial wound healing, decrease the expression of inflammatory cytokines, and increase the expression of trophic factors [10,11]. In prior work, we reported on the development of a biocompatible hyaluronate hydrogel crosslinked *via* visible light-induced thiol-ene reaction [12].

Although photocrosslinking is efficient and highly controllable, its application for in situ gel formation on the cornea poses certain limitations, including the need for an external light energy source, the requirement of a photo-initiator, and the presence of reactive side products. Here, we used the bio-orthogonal strain-promoted azide-alkyne cycloaddition (SPAAC) reaction to crosslink hyaluronate and collagen under ambient conditions without the need for light, heat, photo-initiators, or any other chemical initiators or catalysts. This dual component hydrogel integrates the cell-adhesive nature of collagen and the growth-promoting properties of HA. We systematically studied the crosslinking parameters that yield a highly transparent HA-collagen hydrogel with physical and optical properties comparable to those of corneal stroma. To study the hydrogel's corneal stromal wound healing effects *in vivo*, we used a keratectomy model in rabbits using a custom vacuum trephine. Our results demonstrate that the in situ-forming, bio-orthogonally crosslinked HA-collagen hydrogel is a promising repair matrix for the wounded cornea..

2. Materials and methods

2.1. Materials

Dibenzocyclooctyne-sulfo-*N*-hydroxysuccinimidyl ester (DBCO-sulfo-NHS), dimethyl sulfoxide (DMSO), sodium hydroxide solution (1.0 n), agar, insulin, Triton-X, trypan blue solution, hyaluronidase type VI-S, collagenase type I, and resazurin based *in vitro* toxicology assay kit were purchased from Sigma-Aldrich (St. Louis, MO, USA). Phosphate-buffered saline (PBS) pH 7.4, 10 × PBS, Slide-A-Lyzer dialysis kit (3.5 k MWCO), collagen I bovine protein solution (5 mg/mL), epidermal growth factor (EGF) recombinant human protein, fetal bovine serum (FBS), keratinocyte-serum free media (KSFM), bovine pyruvate extract (BPE), ITS Premix Universal Culture Supplement, trypsin, live/dead viability/cytotoxicity staining kit, paraformaldehyde (PFA), 5% normal goat serum, Alexa Fluor Phalloidin 488, Alexa Fluor 647-*N*-hydroxysuccinimidyl ester, and Alexa Fluor 546 secondary antibody were purchased from Thermo Fisher Scientific (Waltham, MA, USA). Azido-poly (ethylene glycol)$_5$-*N*-hydroxysuccinimidyl ester (azido-PEG5-NHS) was purchased from BroadPharm (San Diego, CA, USA). Hyaluronate amine (40–50% degree of substitute) was purchased from Creative PEGWorks (Durham, NC, USA).

2.2. Hyaluronate-collagen hydrogel synthesis

First, to make HA-azide, 20 mg/mL hyaluronate amine in distilled deionized water was pH neutralized using a neutralization solution at a 1:10 ratio. The neutralization solution was 10X PBS containing 50 mM sodium hydroxide. Next, we made 1000 mg/mL azido-PEG5-NHS with DMSO and added 20.52 μL into 1 mL neutralized HA-amine solution. The mixture was rotated for 2 h at 4 °C. To make fluorescent hydrogel for better visualization *in vivo*, Alexa Fluor 647 was conjugated to the azide-conjugated hyaluronate amine. Specifically, Alexa Fluor 647-*N*-hydroxysuccinimidyl ester was added into 1 mL azide-conjugated hyaluronate amine and incubated for 2 h at 4 °C. Last, azide- or both azide- and 647-conjugated hyaluronate amine was dialyzed using a Slide-A-Lyzer dialysis kit overnight at 4 °C in PBS and then lyophilized.

For Col-DBCO conjugation, type I bovine collagen was pH neutralized using a solution of 1.0 M sodium hydroxide solution, distilled deionized water, and 10X PBS in a 3:57:20 ratio. The 5 mg/mL collagen solution was mixed with the neutralization solution in 3:2 ratio so that the final concentration of collagen was 3 mg/mL. Then, 2 mg DBCO-sulfo-NHS was dissolved in 20 μL PBS, and quickly mixed 8.52 μL DBCO-sulfo-NHS solution with 1 mL neutralized collagen. The mixture was incubated for 2 h at 4 °C. DBCO-conjugated collagen was used fresh and without dialysis unless specified.

To make varying concentrations of hyaluronate-collagen hydrogels *via* SPAAC click reaction, lyophilized HA-azide or HA-azide-647 were dissolved in PBS at 10, 30, or 50 mg/mL, and the Col-DBCO were diluted to 2 or 1 mg/mL with PBS. HA-azide was then mixed with Col-DBCO at a 1:1 ratio *via* pipetting and formed a hydrogel at ambient temperature.

2.3. Hydrogel characterization

The conjugated DBCO and azide groups were quantified by UV–vis absorbance spectra from 270 nm to 350 nm (Tecan Microplate Reader) as DBCO groups resulted in characteristic intense absorbance peaks at approximately 290 and 310 nm, and azide groups resulted in a characteristic absorbance peak at around 285 nm [13]. DBCO-sulfo-NHS and azido-PEG5-NHS were dissolved in PBS at known concentrations and used as standards. Neutralized collagen and hyaluronate amine were used as controls.

The transmittance of the hydrogel was calculated based on the measured absorbance. First, 100 μL of hydrogels were formed within the wells of a 96-well plate. Absorbance of the hydrogels was measured between 200 nm and 1000 nm (Tecan Microplate Reader) and the blank used was PBS. The transmittance was calculated using the relationship $T\ (\%) = 1/10^{A} \times 100$, where A is the absorbance.

The refractive index of hydrogels was measured with a digital refractometer (HI96800, Hanna Instruments). The machine was calibrated with double distilled water. Surface focal power (D_s) of the hydrogels was calculated with the formula $D_s = (n-1)/r$, where n is the measured refractive index and r is the radius of curvature which is 8 mm for human.

The storage and loss moduli of the collagen gels were evaluated using an ARES-G2 rheometer (TA Instruments, New Castle, DE, USA). For in situ measurements, 50 μL HA-azide and 50 μL Col-DBCO were added and mixed on the stage, and a 25-mm parallel plate was used. To measure storage and loss moduli of cornea buttons, rabbit cornea buttons were created with an 8-mm biopsy punch, and then the epithelium and endothelium layers were removed. A wound was created with a 3.5-mm biopsy punch and spatula. The wound was either filled with PBS or 5 μL hydrogel. An 8-mm parallel plate was used for the cornea buttons. Time sweeps were performed at 25 °C for 1 h at 1% strain and 1 Hz oscillatory frequency. Frequency sweeps were performed from 0.1

to 10 Hz with a fixed 1% strain.

In vitro degradation of hydrogel was performed in the presence of 10 U/mL of collagenase, 10 U/mL of hyaluronidase, or a combination of 10 U/mL of collagenase and 10 U/mL of hyaluronidase in PBS at 37 ˚C on an orbital shaker [14]. Hydrogels (200 μL each) were preswollen in PBS (pH 7.4) overnight. At desired timepoints, the gel was removed from the degradation buffer, blotted dry, and weighed. The percent of degraded gels was determined by the following formula: degraded (%) = 100 – W_t/W_0 (W_0 and W_t are the initial weight and weight at time t). Gels soaked in PBS were used as the negative control.

Scanning electron microscope (SEM) imaging was used to examine the morphology and interface between the gel and corneal stroma. The samples were flattened on silicon wafers, flash frozen with liquid nitrogen, and then lyophilized to remove the water. The lyophilized samples were fixed on top of the sample holder with silver paste and then coated with Au/Pd (60:40 ratio). The samples were imaged with an Apreo S LoVac SEM (Thermo Fisher Scientific) at 2–5 kV and 13–50 pA.

2.4. Corneal epithelial cell culture

Corneal epithelial cells (ATCC® CRL-11135™) were used to test the hydrogels' cytocompatibility. Cells were cultured in Keratinocyte-Serum Free Medium supplemented with 0.05 mg/mL bovine pituitary extract, 5 ng/mL epidermal growth factor, 500 ng/mL hydrocortisone, and 5 μg/mL insulin. Cells were incubated under standard conditions and the medium was refreshed every other day. Cells were passaged at 80% confluency with Trypsin-EDTA solution.

2.5. Cytocompatibility

Cytocompatibility of HA-azide and Col-DBCO was evaluated with corneal epithelial cells *via* a Resazurin based cytotoxicity assay (Sigma-Aldrich). Corneal epithelial cells were seeded into 96 well plates at a density of 10,000 cells/well and incubated overnight. The old cell medium was then replaced with fresh medium containing the individual hydrogel components (either HA-azide of 25, 12.5, 1.25, and 0.125 mg/mL or Col-DBCO of 1.5 mg/mL). After 4 h incubation, the medium was aspirated, and resazurin solution was added to cell medium at a ratio of 1:10. After 4 h, the fluorescence was read at an excitation wavelength of 545 nm and emission wavelength of 590 nm.

Additionally, we tested the cytocompatibility of the formed hydrogel with a Calcein AM/Ethidium homodimer-I live/dead assay (ThermoFisher). Hydrogel were formed on a glass slide and then placed inside a 12-well plate. Then, 150,000 corneal epithelial cells were added into the 12-well plate to cover the gel. Cells were imaged on days 0, 1, 2, and 4. For day 0, cells were allowed 3 h to adhere to the surface of the gel. Calcein AM was added at a 1:1000 ratio, and Ethidium homodimer-1 was added at a 1:500 ratio to cell media and added to the cells. Cells were incubated for 45 min after adding the dyes, and imaging was done under the conditions of 37 ˚C and 5% CO_2. Live/dead counts were analyzed using the ImageJ counter feature.

2.6. Organ culture

Fresh rabbit eyes were obtained from Vision Technologies (Glen Burnie, MD). Keratectomy was performed using a customized 3.5-mm vacuum trephine to make a circular cut. The stromal tissue in the wound area was then removed with a spatula. Next, the entire cornea with an approximately 1-mm scleral rim on the edge was removed from the globe. The cornea was sterilized in beta-iodine and 1X PBS containing 1% penicillin/streptomycin. The cornea was immediately transferred onto preformed agar plugs to maintain normal culture and nutritional support. Agar plugs were made of a 1:1 mixture of serum--free medium containing double strength antibiotics and 2% agar in distilled water. The agar plugs were made in polydimethylsiloxane (PDMS) molds. The culture medium used was DMEM/F-12 containing 120 μg/mL penicillin G, 200 μg/mL streptomycin sulfate, and ITS premix universal culture supplement. Samples were incubated at 37 ˚C in 5% CO_2, and the medium was changed every 2 days. At day 4, corneas were fixed in 4% PFA and cryosectioned for immunofluorescence staining or in 10% formalin and sectioned for histochemical staining.

2.7. In vivo lamellar keratectomy studies

Adult New Zealand white rabbits were used in this study. Animal experiments were designed to conform with the ARVO statement for the Use of Animals in Ophthalmic and Vision Research and were reviewed and approved by the Stanford University Institutional Animal Care and Use Committee. All anesthesia techniques were performed by the veterinary service center (VSC) at Stanford University. Prior to surgery, one drop of proparacaine hydrochloride ophthalmic solution was added to the eye receiving treatment. Lamellar keratectomy was performed on the right eye using a 3.5-mm customized vacuum trephine to create a deep circular cut and a spatula to remove the collagen fibril layers. 5 μL of premixed HA-azide and Col-DBCO was applied to the wounded site and allowed to gel in situ. A contact lens was applied to protect the hydrogel from scratching. A tarsorrhaphy was then performed to prevent agitation by the animal and to help keep the contact lens and gel in place. Ofloxacin ophthalmic solution was applied daily to prevent infection and to retain moisture of the eye. On days 4 and 7, the tarsorrhaphy was removed for eye examination: photograph with a Paxos smartphone-based ophthalmic camera adapter [15] and optical coherence tomography (OCT). On day 7, the rabbits' eyes were enucleated, fixed in 4% PFA, and cryosectioned for imaging.

2.8. Statistical analysis

All data are expressed as the mean ± standard deviation. Each experiment was repeated at least 3 times. A two-tailed Student's *t*-test was used for significance, and p values < 0.05 were considered significant. Data means, standard deviations, and p values were calculated in Microsoft Excel 2016.

3. Results and discussion

3.1. Synthetic strategy for highly transparent hyaluronate-collagen hydrogels

To make the hyaluronate-collagen network *via* SPAAC reaction, there are two possible modification strategies: modify hyaluronate with azide (abbreviated as HA-azide hereafter) and collagen with DBCO (abbreviated as Col-DBCO hereafter) or the opposite. We found that the first strategy was superior to the second one due to significant differences in transparency of their products. DBCO-modified hyaluronate (HA-DBCO, 20 mg/mL), one of the mid-products of the second strategy, was translucent when the initial molar ratio of DBCO to amine was 1:4, and it became completely opaque when this ratio increased to 1:2 (Fig. S1a). When HA-DBCO was mixed with collagen-azide in varying ratios, the transmittance of the resulting hydrogels decreased as the amount of HA-DBCO was increased (Fig. S1b).

On the other hand, both HA-azide (20 mg/mL) and Col-DBCO (10 mg/mL) were transparent, resulting in a more transparent hydrogel than HA-DBCO and Col-azide (Fig. S1b). Hence, we chose this strategy to make hyaluronate-collagen hydrogel (Fig. 1). Specifically, the amidated hyaluronate and collagen were modified with azide and DBCO respectively *via* N-hydroxysuccinimidyl ester assisted amide reaction (Fig. 1 a, b). Conjugation of DBCO and azide were quantified using absorbance spectra. DBCO has intense absorbance peaks at approximately 290 and 310 nm, while collagen does not (Fig. S2a) [13]. As shown in Fig. S2b, there was a linear relationship between the DBCO

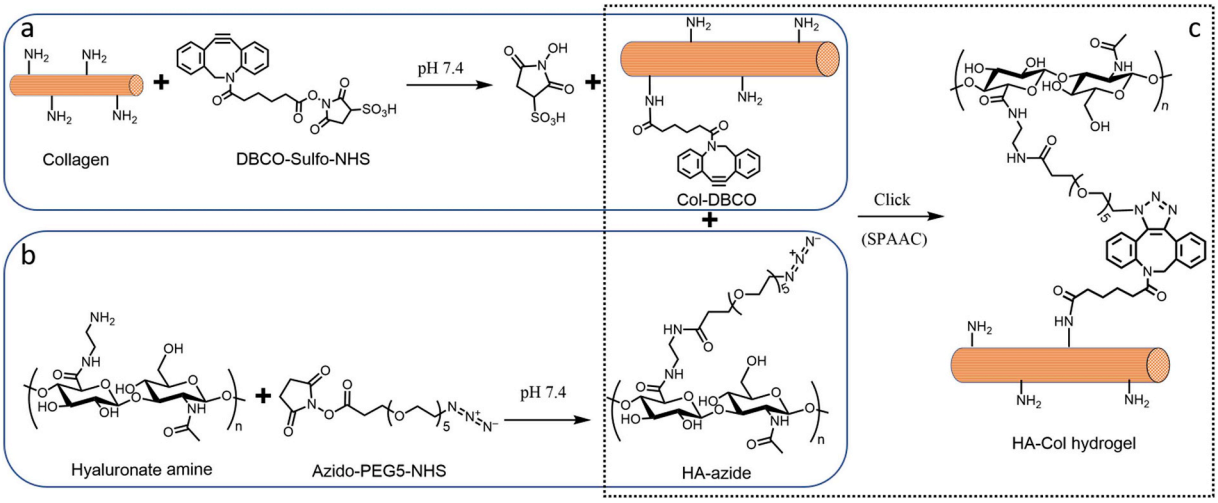

Fig. 1. Hyaluronate-collagen hydrogel crosslinked *via* strain-promoted azide-alkyne cycloaddition (SPAAC). (a–c) Reaction scheme of the hydrogel formation. (a) Primary amine groups on collagen react with dibenzocyclooctyne-sulfo-N-hydroxysuccinimidyl ester to form collagen-DBCO (Col-DBCO). (b) Amidated hyaluronate react with azido-PEG5-NHS and formed hyaluronate-azide (HA-azide). (c) The SPAAC reaction between DBCO and azide groups formed hyaluronate-collagen networks without producing any byproducts.

concentration and its absorbance at 306 nm. We calculated the conjugated DBCO on Col-DBCO and found that there were 12.5 ± 7.1 nmol conjugated DBCO per mg of Col-DBCO. The primary amine groups per collagen was calculated to be approximately 269 nmol/mg collagen [9]. Therefore, the degree of substitution of DBCO was 4.63%. Similarly, the azide has a featured absorbance peak at around 285 nm, and it is linearly dependent on the azide concentration (Fig. S2c, d). There were 19.6 ± 2.5 nmol conjugated azide per mg of HA-azide and the degree of substitution of azido was 1.66%.

The dialyzed HA-azide was then mixed with Col-DBCO, crosslinked through SPAAC reaction, and produced the hyaluronate-collagen hydrogel (Fig. 1c). The absorbance at 310 nm dropped dramatically upon mixing of HA-azide and Col-DBCO (Fig. S2e), which was likely due to the crosslinking between DBCO and azide [13]. This result indicated that the SPAAC reaction was initiated as soon as the gel components were mixed. Further analysis of the absorbance changes showed that 17%, 48%, 50%, and 54% of DBCO crosslinked within 0, 10, 30, and 60 min, respectively (Fig. S2f).

3.2. Physical and optical properties of hydrogels

We studied the mechanical properties of hydrogels with different polymer concentrations by mixing 10, 30, or 50 mg/mL HA-azide with 1, 2, or 3 mg/mL Col-DBCO at 1:1 vol ratio. The highest initial Col-DBCO concentration was set at 3 mg/mL, which led to a final collagen concentration of 1.5 mg/mL, because according to our previous study, a collagen concentration of 1.5 mg/mL resulted in improved re-epithelialization on cornea than higher concentrations did [9]. When the Col-DBCO was kept at 3 mg/mL, storage and loss moduli of hydrogels increased as the HA-azide increased from 10 to 50 mg/mL (Fig. 2a). Similarly, both moduli also increased when the Col-DBCO content increased from 1 to 3 mg/mL while the HA-azide concentration was kept constant at 50 mg/mL (Fig. 2b).

Noticeably, the hydrogel with 15 mg/mL HA-azide and 1.5 mg/mL Col-DBCO (HA30-Col 3) showed higher storage and loss moduli than hydrogel with 25 mg/mL HA-azide and 0.5 mg/mL Col-DBCO (HA50-Col1), even though the first hydrogel had a lower polymer concentration (Fig. 2c). Because the azide-DBCO coupling reaction occurs with an exact 1 to 1 stoichiometry, the maximum ideal amount of network crosslinking will occur when the azide-to-DBCO ratio is 1:1, while having a large excess of either azide or DBCO will result in less efficient network crosslinking. Absorbance spectra showed that HA30-Col3 had 295 nmol azide and 385 nmol DBCO per mL of total hydrogel solution (the azide-to-DBCO ratio was 0.77); and HA50-Col1 had 491 nmol azide and 128 nmol DBCO per mL of total hydrogel solution (the azide-to-DBCO ratio was 3.84) (Fig. S2 a, b). This indicated that HA30-Col3 had more efficient crosslinking than HA50-Col1 resulting in a more networked structure. Therefore, as expected, the hydrogels' moduli depended not only on the polymer concentration but also on the density of crosslinks within the network.

The stiffest hydrogel (HA50-Col3) contained final concentrations of 25 mg/mL HA-azide and 1.5 mg/mL Col-DBCO, which equaled to 2.65% (w/v) polymer and 97.35% water (Fig. 2c). Its azide-to-DBCO ratio was approximately 1.3. The excess azide relative to DBCO likely speeds up the SPAAC reaction [16]. This hydrogel is significantly stiffer and more closely mimics corneal stroma compared to our previously reported SPAAC-crosslinked collagen-only hydrogel [9]. *In situ* rheology studies indicated that the hydrogel started to form before the beginning of the rheology measurements, because the measured storage modulus was already higher than the loss modulus [16]. The storage modulus reached half maximum in approximately 3 min and plateaued in approximately 40 min (Fig. 2d). This duration is suitable for an *in-situ* gel application procedure.

We also directly measured the mechanical properties of the stiffest hydrogel HA50-Col3 in conjunction with rabbit corneal buttons as a defect-filling matrix. To exclude the negative effect of broken collagen fibrils [17], we used intact cornea buttons (red circled) and wounded cornea buttons (blue circled) as positive and negative controls, as shown in Fig. 2e (inset). The storage and loss moduli of all samples increased as frequency increased (Fig. 2e). Both the storage and loss moduli of wounded cornea buttons were around 20% of the intact cornea button. After filling with the stiffest hydrogel (HA50-Col3), the moduli increased to around 55% of the intact cornea button (Fig. 2f).

The hyaluronate-collagen hydrogels also showed excellent optical properties, making them suitable as corneal stromal substitutes. First, higher transparency is desired to let more light pass through the treated cornea and enter the patient's eye. According to literature, the human cornea has a transmittance over 95% in the spectral range from 380 to 800 nm, which is due to the highly ordered assembly of collagen fibrils [18]. The hydrogels we developed in this work had high transparency that was comparable to the cornea: all the hyaluronate-collagen hydrogels with different polymer contents showed a transmittance over 94% from 380 nm to 410 nm and over 95% between 410 nm and 800 nm (Fig. 3a). As a control, the mixture of 25 mg/mL hyaluronate-

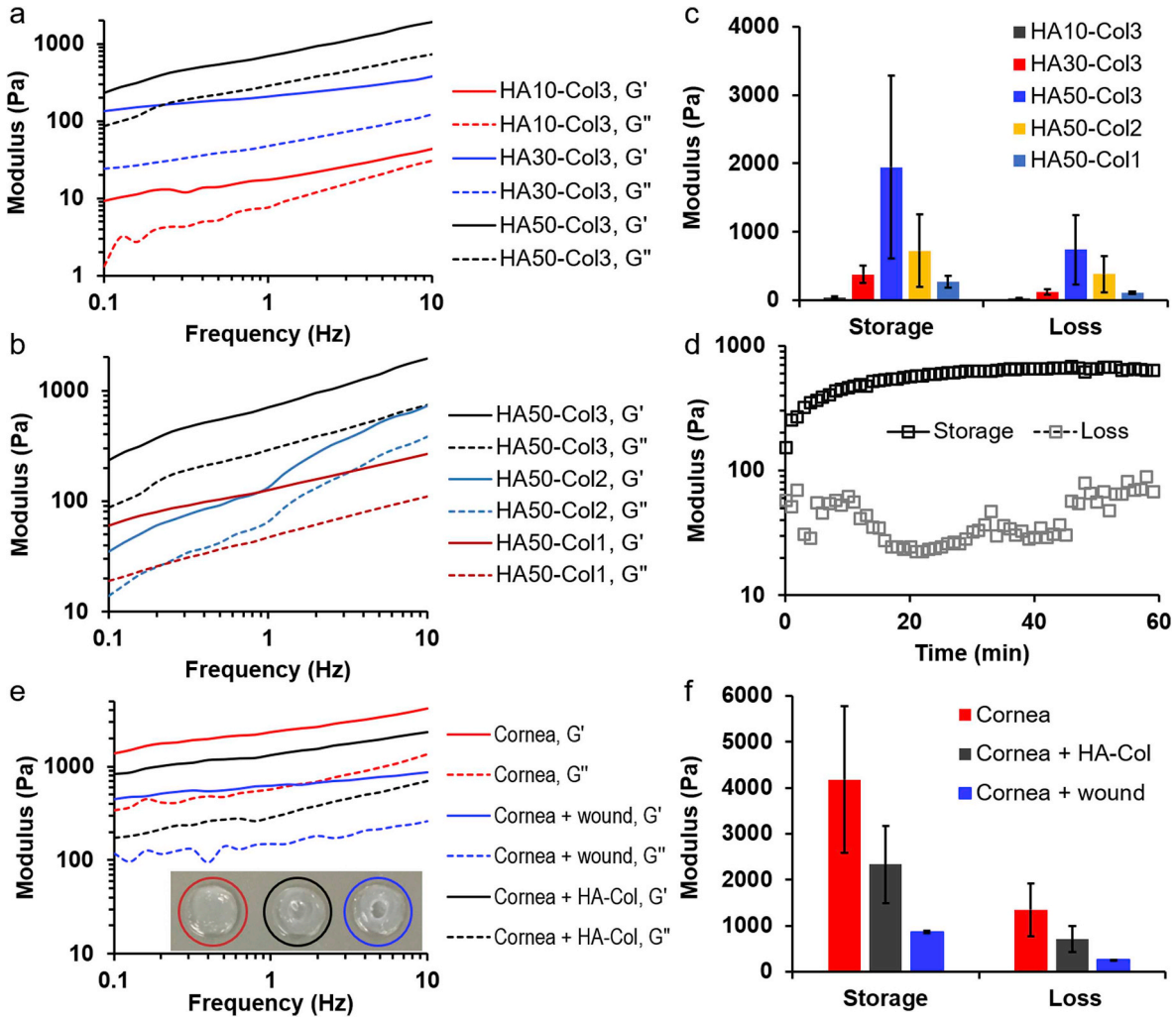

Fig. 2. Mechanical properties of hyaluronate-collagen hydrogels. (a & b) Storage and loss moduli of hydrogels increased as the frequency increased. The samples had different hyaluronate (HA) and collagen (Col) content, numbers are the polymer concentration (mg/mL) prior to mixing at a 1:1 vol ratio. G′ is storage modulus and G″ is loss modulus. (c) Hydrogel with a final concentration of 25 mg/mL hyaluronate and 1.5 mg/mL collagen (HA50-Col3) showed the highest storage and loss moduli at a frequency 10 Hz. (d) Moduli of hydrogel HA50-Col3 as a function of time at the beginning of gelation. (e) Storage and loss moduli of intact and wounded cornea buttons as well as wounded cornea buttons with the stiffest hydrogel from (c). (f) The hydrogel HA50-Col3 increased the storage and loss moduli of wounded cornea buttons.

azide and 1.5 mg/mL collagen without DBCO had a much lower transmittance, lower than 80% between 380 nm and 410 nm (Fig. 3a). Hence, the high transparency of hyaluronate-collagen hydrogel was due to the SPAAC crosslinking between hyaluronate and collagen, which presumably disrupts the aggregation of distinct hyaluronate and collagen gel microdomains that can scatter visible light. These data are consistent with other crosslinked hydrogel networks that form through the covalent bonding of two dissimilar polymers [19].

Another crucial optical property of a corneal substitute is its focal power, which is defined as the reciprocal of focal length and indicates the degree to which the cornea substitutes converge light. The average total corneal power of normal human eyes is around 43 m^{-1} [20]. The

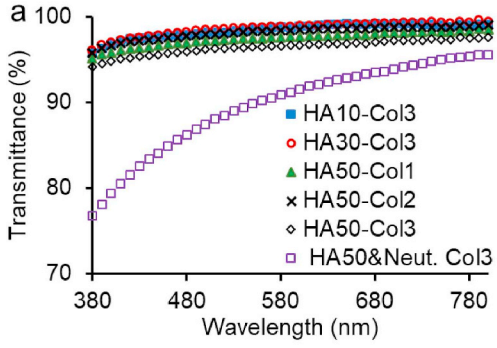

b

Samples	Refractive index (n)	Surface focal power (Ds, m^{-1})*	Surface focal Length (Fs, mm)*
HA50-Col1	1.3431	42.9	23.3
HA50-Col2	1.3428	42.8	23.3
HA50-Col3	1.3423	42.8	23.4
HA30-Col3	1.3402	42.5	23.5
HA10-Col3	1.3403	42.5	23.5
Human cornea	1.3760#	47.0	21.3

* Ds=(n-1)/r, r: radius of curvature (8 mm for human).
# Adapted from literature.

Fig. 3. Optical properties of hyaluronate-collagen hydrogels. (a) Transmittance of SPAAC crosslinked hyaluronate-collagen hydrogels were much higher than non-crosslinked hydrogel (HA50 & Neut. Col 3). (b) Refractive index, surface focal power, and surface focal length of the hydrogels and human cornea for comparison.

corneal surface power was determined by the corneal curvature radius and refractive index [21]. The average refractive index of the human cornea is reported to be 1.376. The refractive index of the hyaluronate-collagen hydrogel ranges from 1.340 to 1.343 (Fig. 3b). The surface focal power of the hydrogels was calculated using 8 mm as the radius of curvature. Results showed that the focal power of hydrogels was slightly lower than the human cornea, and the focal length difference between the hydrogels and human cornea was around 2 mm. (Fig. 3b).

The focal power or focal length can be matched to naïve cornea by changing the radius curvature. *Ex vivo* optical coherence tomography (OCT) showed that the curvature of the central cornea could be adjusted by changing the volume of the applied hydrogel (Fig. S3). The decreased radius curvature could compensate the slightly lower refractive index of the hydrogel to achieve the same focal length. Moreover, given that the gel can be used in conjunction with a contact lens, this underpowering can be overcome with either a higher power contact lens (e.g. 1.0–5.0 diopters) or by a modified base curve of the contact lens to form a steeper or flatter curvature to the gel as it is formed. Furthermore, additives can be included in the gel to increase its refractive index; if that additive is stromal cells (e.g. keratocytes), then the refractive index of the gel may increase over time as certain biomolecules are produced by those cells, such as the corneal crystallin aldehyde dehydrogenase 3A1 (ALDH3A1) [22].

3.3. Degradation of hydrogel HA50-Col3

The mechanical and optical properties of the hydrogels indicated the stiffest hydrogel had 1.5 mg/mL collagen, which was also the collagen concentration that most optimally promoted cornea re-epithelialization in a different, previously reported hydrogel formulation [9]. Therefore, we focused on this HA50-Col3 hydrogel for all the other tests. First, we studied the *in vitro* degradation profiles of the HA50-Col3 in the presence of collagenase, hyaluronidase, or both enzymes (Fig. 4). Both collagenase and hyaluronidase exist naturally in the body. The percentage of degraded gel was plotted against the degradation time. The HA50-Col3 gel degraded most rapidly in the presence of collagenase and hyaluronidase: approximately 30%, 90%, and 100% of the gel degraded in 10 U/mL of collagenase, 10 U/mL of hyaluronidase, and a combination of 10 U/mL of each enzyme after 24 h, respectively (Fig. 4). The degradation rate was lower in the presence of hyaluronidase alone and collagenase alone, with hyaluronidase resulting in faster degradation than collagenase. These results together indicate that the hydrogel network is held together by a combination of collagen and HA, rather than just one of the two macromers. The HA50-Col3 gel did not degrade in PBS at 37 °C over 24 h, demonstrating gel stability in the absence of enzymes.

3.4. Cytocompatibility, bio-integration, and re-epithelialization capacity of hydrogel HA50-Col3

Next, we studied the cytocompatibility of the hydrogel with corneal epithelial cells. Although hyaluronate and collagen are non-toxic to humans, the conjugated functional groups might be less well tolerated [23]. A resazurin based viability assay showed that collagen-DBCO at 1.5 mg/mL was tolerated by cells, while the hyaluronate-azide at 25 mg/mL decreased the cell viability to 80%. The HA-azide at lower concentrations, however, did not show any significant toxicity (Fig. 5a). The decreased cytocompatibility of 25 mg/mL HA-azide is likely due to the extremely high dose of the dangling azide (490 μmol/L) [24]. The biocompatibility of 25 mg/mL HA-azide should be increased dramatically once the azide groups have crosslinked with DBCO.

To verify our hypothesis, we tested the cytocompatibility of HA50-Col3 with Calcein AM/Ethidium homodimer-I live/dead assay on different days. Of note, HA50-Col3 gels have a theoretical azide-to-DBCO ratio of 26.1, leading to many unreacted azide groups, even if all DBCO groups were reacted. To prevent potential toxicity due to this excess azide, unconjugated DBCO from the original Col-DBCO conjugation reaction was simply mixed with HA-azide to yield a final theoretical azide-to-DBCO ratio of 1.3 We hypothesized this addition of unconjugated DBCO would quench the dangling azide groups that might cause toxicity [24]. Very few dead cells were seen after the corneal epithelial cells were incubated on the hydrogel for 4 days, and the living cells were spreading on the top of the gel (Fig. 5b). The survival of corneal epithelial cells on the hydrogel was 93.3% ± 3.7%, 91.3% ± 8.1%, 96.4% ± 4.6%, and 96.3% ± 5.5% on days 0, 1, 2, and 4, respectively (Fig. 5c). There was no significant decrease of survival over this period, indicating excellent cytocompatibility of HA50-Col3.

The HA50-Col3 hydrogel was found to be able to support the re-epithelialization of wounded corneas in an *ex vivo* organ culture study. We performed an anterior lamellar keratectomy on enucleated rabbit eyes and filled the defects with the gels, forming them in situ on the wound bed. We studied the integration of this hydrogel with corneal stromal tissues. SEM images showed that the hydrogel filled the corneal wound without any detectable fissures at the hydrogel-stromal interface on a 5,000× magnified view (Fig. 5d and e), which bodes well for the hydrogel's potential for biointegration with corneal stroma.

Then, we tested the *ex vivo* re-epithelialization capacity of the gels placed within the defects in the corneal stroma. The epithelium on the keratectomy area was completely removed, and a superficial layer of

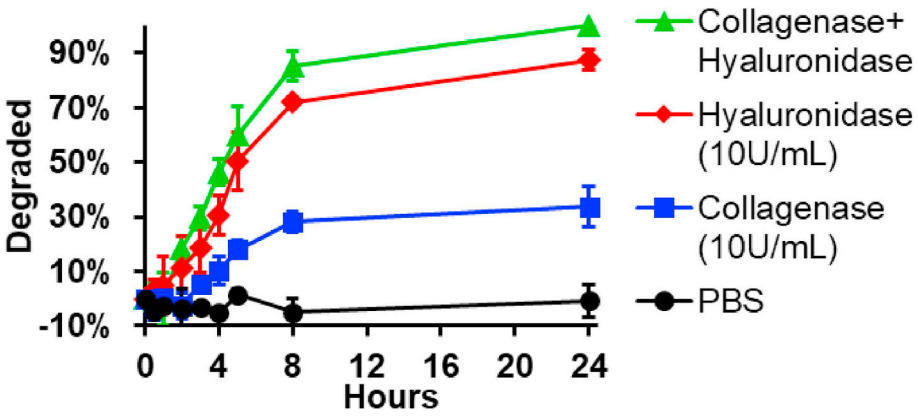

Fig. 4. *In vitro* degradation of HA50-Col3 in presence of collagenase and hyaluronidase. The HA50-Col3 degraded the fastest and most when both enzymes were present. No degradation of the gel was detected in PBS only within 24 h.

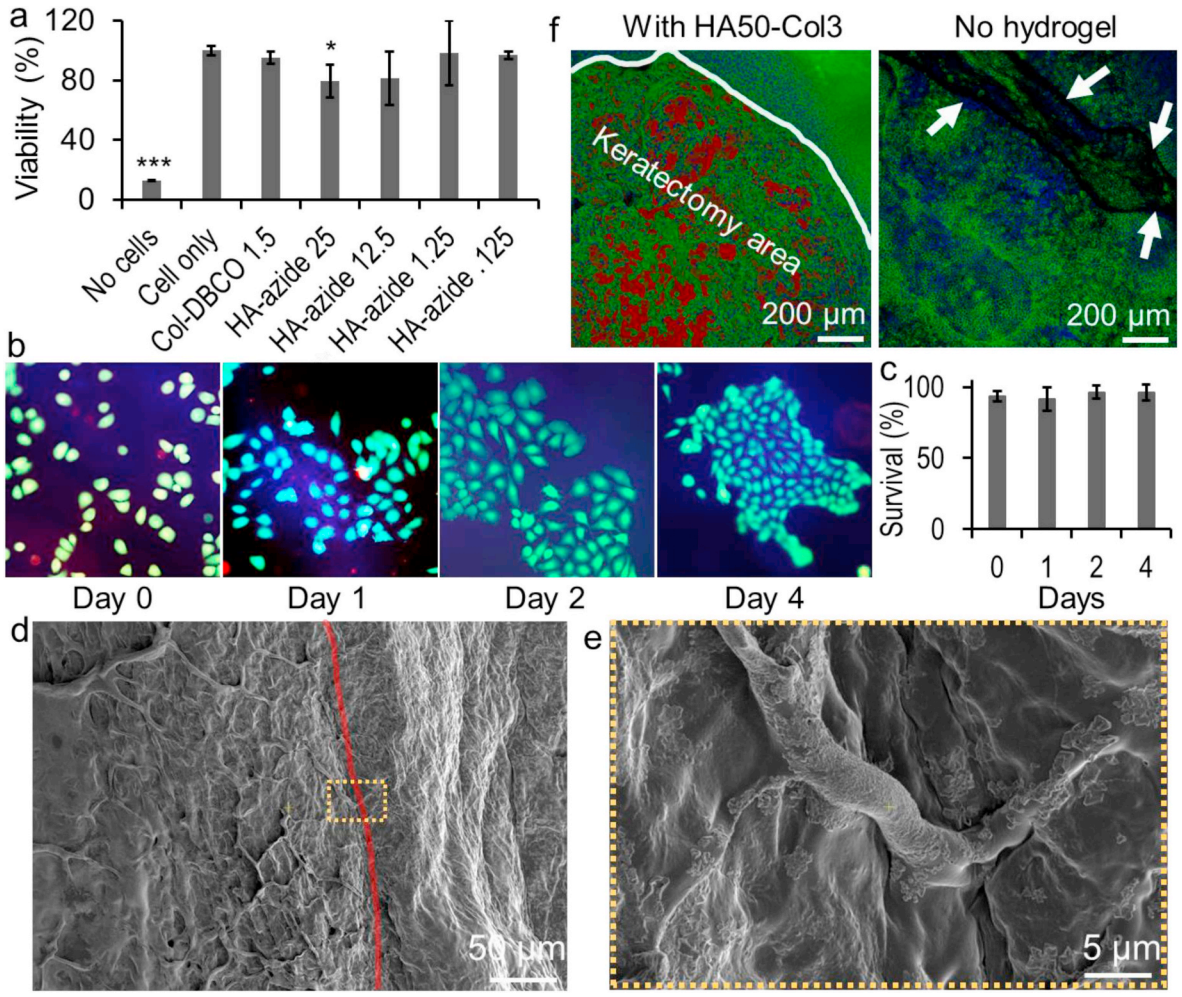

Fig. 5. Cytocompatibility, bio-integration, and re-epithelialization capacity of HA50-Col3 hydrogel to corneal epithelial cells. (a) Cell viability assay showed that collagen-DBCO 1.5 mg/mL was cytocompatible. The HA-azide at low concentrations were cytocompatible, but HA-azide at 25 mg/mL decreased the cell viability to 80%. The decrease is significant when compared to the cell only group. (*$p < 0.05$, ***$p < 0.005$, 2-tail homoscedastic *t*-test). The error bars represent standard deviation of four replicates. (b) *In vitro* live/dead assay showed that corneal epithelial cells could grow on top of the HA50-Col3 with a high survival. The hydrogel was modified with Alexa Fluor 647 (blue). Green and red showed live and dead cells, respectively. (c) Quantification of cell survival on top of HA50-Col3 hydrogel on different days based on the live/dead assay. Error bars represent standard deviations of at least five fields of views from different replicates. (d) SEM image of HA50-Col3 filling the keratectomy defect on corneal stroma. The red line roughly indicates the interface between the hydrogel and the corneal stroma. (e) Higher magnified SEM image showing the dotted area in (d). There is no detectable gap or separation between the hydrogel and the adjacent cornea, which indicates good physical apposition between the gel and the corneal stroma. (f) Top view of wounded cornea treated with and without HA50-Col3 hydrogel in an *ex vivo* organ culture-based keratectomy wound model. HA50-Col3 promoted the re-epithelialization. The hydrogel was modified with Alexa Fluor 647 and is shown in red. Green and blue showed the F-actin and nuclei, respectively. The white arrows point to gaps in the epithelial layer on the wounded cornea without hydrogel treatment. (For interpretation of the references to colour in this figure legend, the reader is referred to the Web version of this article.)

stroma was removed. Then, the wound was filled with the hydrogel HA50-Col3 immediately after mixing the HA-azide 50 mg/mL and Col-DBCO 3 mg/mL at a 1:1 vol ratio. To better visualize the hydrogel, we modified the HA-azide with a fluorophore (Alexa Fluor 647). Epithelial cell coverage was imaged from a top view of wounded corneas, both with and without hydrogel treatment (Fig. 5f). The hydrogel was almost completely covered by cells after four days of incubation, while multiple gaps were seen on the wounded cornea without the hydrogel (Fig. 5f). Cell migration from the adjacent epithelium over the surface of the HA50-Col3 gel was observed, indicating excellent cell adhesion over the collagen-HA gel. In previous reports, while collagen gels have been shown to support epithelial adhesion, HA-only gels have not. Thus, our collagen-HA gel combines the known cell adhesion properties of collagen with the mechanical and proliferation-promoting benefits of HA [9,12].

3.5. *In vivo* assessment of HA50-Col3 hydrogel in a rabbit anterior lamellar keratoplasty model

To further understand the potential for the HA-Col hydrogel to promote corneal wound healing, *in vivo* studies were performed using a lamellar keratectomy corneal wound model (Fig. 6a). First, the cornea was wounded with a customized 3.5-mm vacuum trephine on the central cornea (Fig. 6b). The wound depth was controlled to be approximately 60% ± 9% (n = 11) of the corneal central thickness. Then, the hydrogel HA50-Col3 was added into the wound immediately after mixing the HA-azide and Col-DBCO. We added 5 μL of the mixture to the wound, because *ex vivo* optical coherence tomography (OCT) showed that the corneal curvature could be restored with approximately 5 μL of hydrogel (Fig. S3). No swelling or contraction of the hydrogel on the rabbit cornea was seen following in situ gel formation

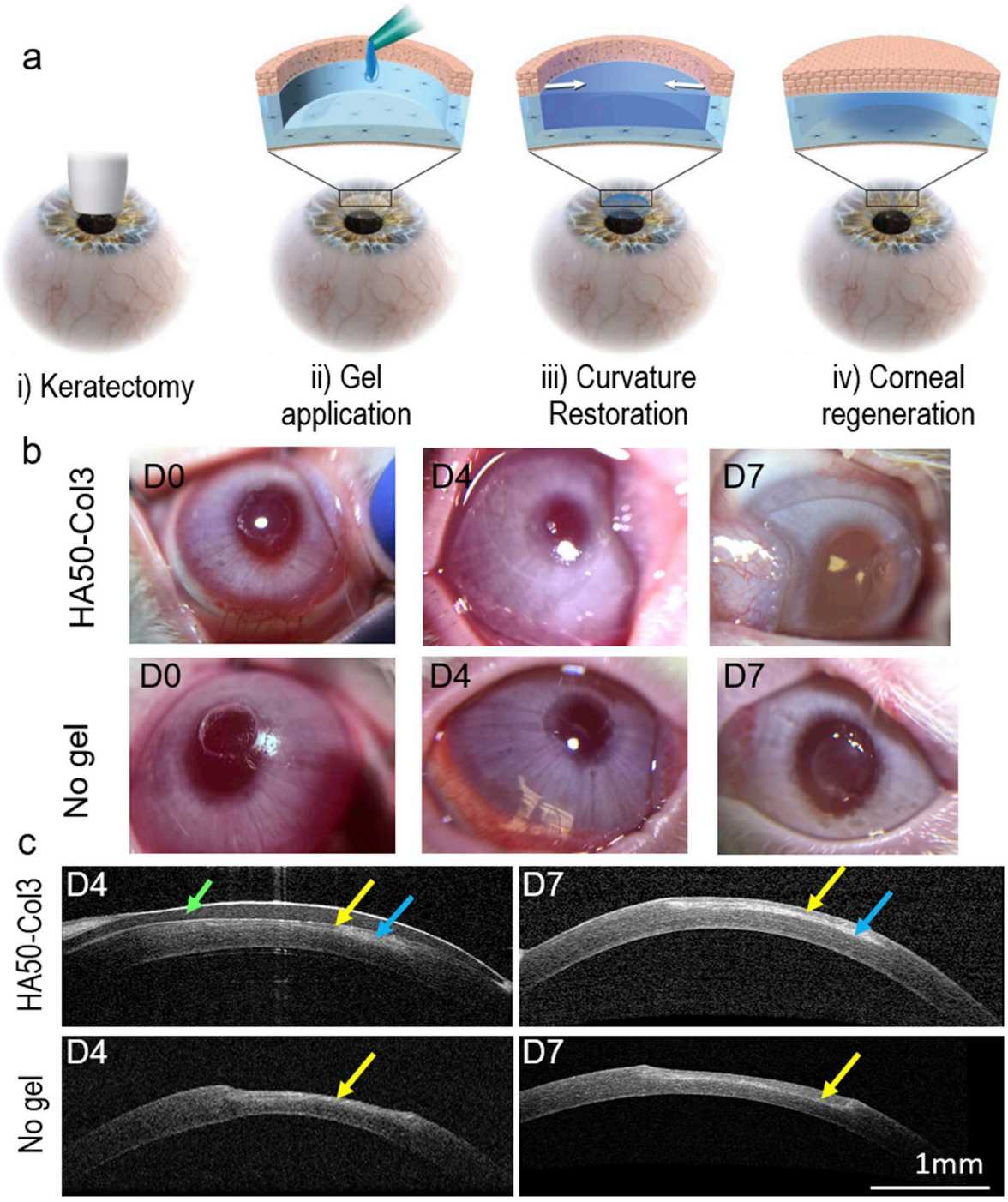

Fig. 6. Application of hydrogel for sutureless repair of corneal wounds. (a) Scheme of the disease model and treatment. The corneal wound was created by anterior lamellar keratectomy using a customized 3.5-mm vacuum trephine. (b) Follow up photos of the rabbit eyes after *in vivo* keratectomy and gel application. (c) Follow-up examination of rabbit eyes with *in vivo* OCT. A contact lens (indicated by the green arrow) was used to protect the hydrogel (blue arrows) from scratching by the animal. The hydrogel HA50-Col3 restored the central corneal curvature. Regenerated epithelium (indicated by the yellow arrows) was seen over the keratectomy area. (For interpretation of the references to colour in this figure legend, the reader is referred to the Web version of this article.)

or during the wound healing over 7 days. The gel was remained clear on the wounded cornea 7 days after gel application (Fig. 6b).

In vivo OCT showed that the wounded cornea applied with HA50-Col3 had a smooth transition between the keratectomy area and adjacent normal cornea, and the corneal curvature was completely restored after one week (Fig. 6c). The average gel thickness was approximately 56 and 50 μm on days 4 and 7, respectively. On the contrary, without gel application, the keratectomy area was thinner than the adjacent cornea and showed a dip in the central cornea (Fig. 6c). Noticeably, there were two layers (approximately 30 and 90 μm) on the central corneal stroma on day 7 for the cornea treated with HA50-Col3. However, for the wounded cornea without hydrogel application, a thin layer (approximately 50 μm) was seen on top of the central cornea on day 4 and it was found to be thickened (to approximately 100 μm) by day 7 (Fig. 6c).

Immunofluorescence staining of the cornea section showed that the

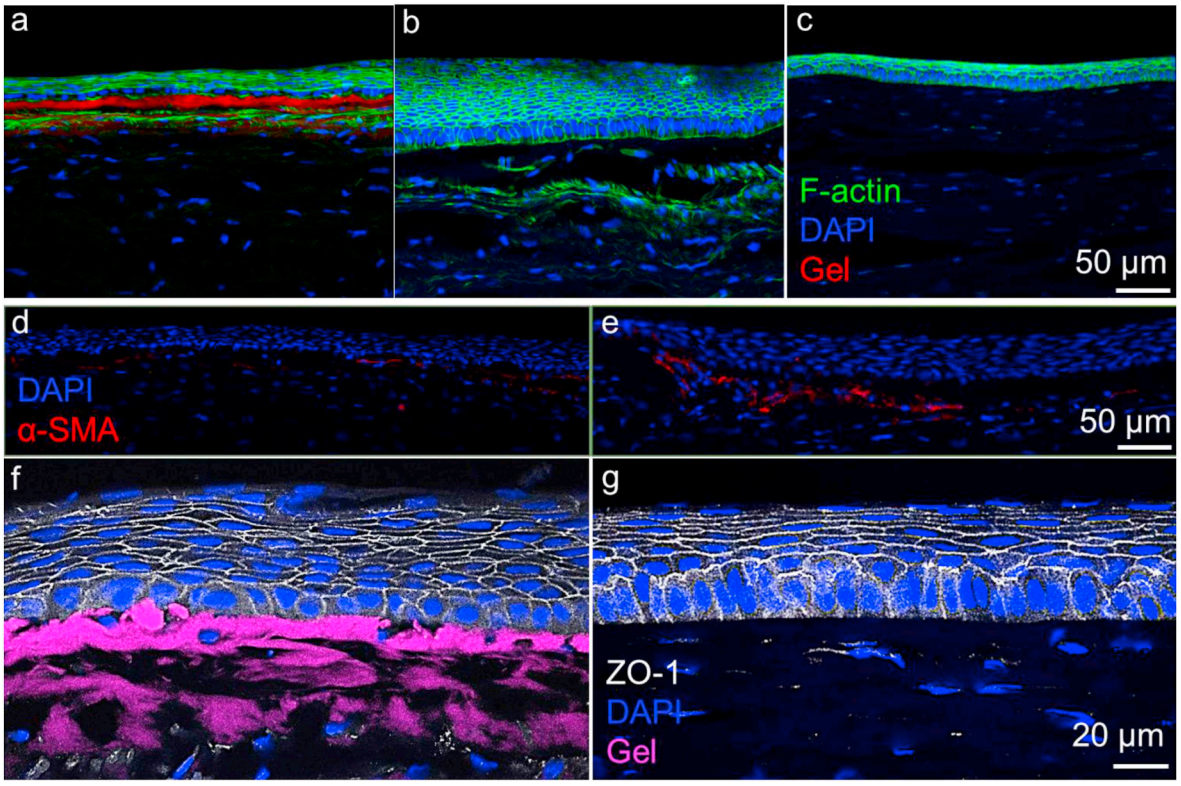

Fig. 7. Immunofluorescence staining of wounded cornea treated with and without hydrogel HA50-Col3. F-actin staining images of (a) wounded cornea treated with HA50-Col3, (b) wounded cornea without gel treatment, and (c) normal cornea. The results show that the HA50-Col3 effectively supports the regeneration of a thin epithelial layer. α-SMA staining images of wounded cornea treated with (d) and without (e) HA50-Col3 gel. The α-SMA staining (red) indicated that HA50-Col3 faciliated reduced expression of α-SMA and may prevent corneal scarring. ZO-1 staining images of (f) wounded cornea treated with HA50-Col3 gel and (g) normal cornea. The HA50-Col3 gel promoted multi-layered epithelialization with excellent tight junction ZO-1 (white) formation (f), similar to that seen in normal corneal epithelium (g). (For interpretation of the references to colour in this figure legend, the reader is referred to the Web version of this article.)

two layers on the corneas treated with HA50-Col3 were regenerated epithelium and the hydrogel respectively (Fig. 7a) and that the layer on the cornea without hydrogel application was hyperplastic epithelium alone (Fig. 7b). On day 7, the hydrogel (modified with fluorophore) was observed under the epithelial cell layers. There were 5–8 layers of epithelial cells, among which the lower layer showed cuboidal basal cells, and the upper layer showed flattened superficial cells (Fig. 7a), which is characteristic of normal epithelium (Fig. 7c) [25]. Without the hydrogel, epithelial hyperplasia was observed, where the epithelium was much thicker than normal and showed 15–20 layers of epithelial cells (Fig. 7b). This is the expected physiological wound healing response to a keratectomy wound or ulcer *in vivo* [26].

Meanwhile, the keratocytes in the keratectomy area were more activated than they were in the normal cornea and wounded cornea treated with the hydrogel. Immunofluorescence staining of alpha smooth muscle actin (α-SMA, ACAT2) showed that the wounded cornea without hydrogel treatment had much more α-SMA expressed at the wound edge than the HA50-Col3 treated cornea (Fig. 7d&e). It is likely that keratocytes close to the wound surface were activated and differentiated into α-SMA-positive myofibroblasts in the wounded cornea [27]. However, HA50-Col3 significantly decreased the expression of α-SMA, which is ideal for avoiding myofibroblast formation and corneal scarring [26]. Immunofluorescence staining of zonula occludens-1 (ZO-1), a tight junction protein in epithelial monolayers, showed comparable expression of ZO-1 in the HA50-Col3 treated cornea and the normal cornea control (Fig. 7f-g) [28]. These images suggest that HA50-Col3 does not cause significant myofibroblast activation and can support tight junction formation within the regenerated epithelial cell layer, which are promising attributes for a corneal stroma substitute candidate material.

4. Conclusion

Here, we report on the development of a bio-orthogonally crosslinked hyaluronate-collagen hydrogel and its *in vitro* and *in vivo* performance as an in situ-forming substitute for corneal stroma. The hydrogel consisted of 97% water and was highly transparent. The material exhibited significantly improved mechanical properties compared to our previously reported SPAAC-crosslinked collagen-only hydrogel [9]. The hyaluronate-collagen hydrogel has a refractive index lower than that of the native cornea, although there are several possible approaches to achieve a synthetic cornea stroma with similar focal power to the native cornea. The hydrogel has potential to improve vision due to the clear, smooth anterior curvature that it forms on corneal wound beds as well as the ability to modulate that curvature during gelation. Its gelation time, which is on the order of minutes, is suitable for therapeutic uses including both point-of-care situations as well as in the operating room. The material crosslinks under ambient, aqueous conditions, requires no light irradiation or any other type of trigger or initiator, and fills stromal defects without the need for sutures. This hydrogel demonstrated excellent cytocompatibility and support for epithelialization *in vitro* and *in vivo*. Future studies are merited to understand the material's capacity to provide functional vision in the treatment of vision-threatening corneal defects.

CRediT authorship contribution statement

Fang Chen: Methodology, Investigation, Formal analysis, Project administration, Writing - original draft. **Peter Le:** Investigation, Validation. **Gabriella M. Fernandes-Cunha:** Investigation. **Sarah C. Heilshorn:** Conceptualization, Writing - review & editing. **David**

Myung: Supervision, Funding acquisition, Writing - review & editing.

Declaration of competing interest

The authors declare the following financial interests/personal relationships which may be considered as potential competing interests: The authors Fang Chen, Gabriella Fernandes-Cunha, David Myung, and Sarah Heilshorn are co-inventors on a related patent application.

Acknowledgements

This work was supported by the National Institutes of Health (National Eye Institute K08EY028176 and a Departmental P30-EY026877 core grant), the Stanford SPARK Translational Research Grant (D.M.), a core grant and Career Development Award from Research to Prevent Blindness (RPB), the Matilda Ziegler Foundation, the VA Rehabilitation Research and Development Small Projects in Rehabilitation Effectiveness (SPiRE) program (I21 RX003179), the Byers Eye Institute at Stanford, and National Science Foundation grant (DMR 1808415 to S.C.H.). Part of this work was performed at the Stanford Nano Shared Facilities (SNSF), supported by the National Science Foundation under award ECCS-1542152. The authors would also like to thank Roopa Dalal (Ophthalmology, Stanford), Sam Baker (VSC, Stanford), Kristina Russano (Ophthalmology, Stanford), and Xin Xia (Ophthalmology, Stanford) for their assistance on this project.

Appendix A. Supplementary data

Supplementary data to this article can be found online at https://doi.org/10.1016/j.biomaterials.2020.120176.

Data availability

The raw/processed data required to produce these findings is available upon request.

References

[1] M.M. Islam, O. Buznyk, J.C. Reddy, N. Pasyechnikova, E.I. Alarcon, S. Hayes, P. Lewis, P. Fagerholm, C. He, S. Iakymenko, W. Liu, K.M. Meek, V.S. Sangwan, M. Griffith, Biomaterials-enabled cornea regeneration in patients at high risk for rejection of donor tissue transplantation, npj Regenerative Medicine 3 (1) (2018) 2.

[2] P. Gain, R. Jullienne, Z.G. He, M. Aldossary, S. Acquart, F. Cognasse, G. Thuret, Global survey of corneal transplantation and eye banking, Jama Ophthalmol 134 (2) (2016) 167–173.

[3] M.R. Dana, Y. Qian, P. Hamrah, Twenty-five–Year panorama of corneal immunology: emerging concepts in the immunopathogenesis of microbial keratitis, peripheral ulcerative keratitis, and corneal transplant rejection, Cornea 19 (5) (2000) 625–643.

[4] M.M. Fernandez, N.A. Afshari, Endothelial keratoplasty: from DLEK to DMEK, Middle East, Afr. J. Ophthalmol. 17 (1) (2010) 5–8.

[5] M. Mobaraki, R. Abbasi, S. Omidian Vandchali, M. Ghaffari, F. Moztarzadeh, M. Mozafari, Corneal Repair and Regeneration: Current Concepts and Future Directions, Frontiers in Bioengineering and Biotechnology 7 (135) (2019).

[6] B.C. Leonard, K. Cosert, M. Winkler, A. Marangakis, S.M. Thomasy, C.J. Murphy, J.V. Jester, V.K. Raghunathan, Stromal collagen arrangement correlates with stiffness of the canine cornea, Bioengineering 7 (1) (2019).

[7] E.S. Sani, A. Kheirkhah, D. Rana, Z.M. Sun, W. Foulsham, A. Sheikhi, A. Khademhosseini, R. Dana, N. Annabi, Sutureless repair of corneal injuries using naturally derived bioadhesive hydrogels, Sci. Adv. 5 (3) (2019).

[8] L. Li, C. Lu, L. Wang, M. Chen, J. White, X. Hao, K.M. McLean, H. Chen, T.C. Hughes, Gelatin-based photocurable hydrogels for corneal wound repair, ACS Appl. Mater. Interfaces 10 (16) (2018) 13283–13292.

[9] H.J. Lee, G.M. Fernandes-Cunha, K.-S. Na, S.M. Hull, D. Myung, Bio-orthogonally crosslinked, in situ forming corneal stromal tissue substitute, Adv. Healthcare Mater. 7 (19) (2018) 1800560.

[10] M.G. Neuman, R.M. Nanau, L. Oruña-Sanchez, G. Coto, Hyaluronic acid and wound healing, J. Pharm. Pharmaceut. Sci. 18 (1) (2015) 53–60.

[11] J. Zhong, Y. Deng, B. Tian, B. Wang, Y. Sun, H. Huang, L. Chen, S. Ling, J. Yuan, Hyaluronate acid-dependent protection and enhanced corneal wound healing against oxidative damage in corneal epithelial cells, J. Ophthalmol. (2016) 2016.

[12] H.J. Lee, G.M. Fernandes-Cunha, D. Myung, In situ-forming hyaluronic acid hydrogel through visible light-induced thiol-ene reaction, React. Funct. Polym. 131 (2018) 29–35.

[13] S.M. Hodgson, E. Bakaic, S.A. Stewart, T. Hoare, A. Adronov, Properties of poly (ethylene glycol) hydrogels cross-linked via strain-promoted alkyne–azide cycloaddition (SPAAC), Biomacromolecules 17 (3) (2016) 1093–1100.

[14] S. Suri, C.E. Schmidt, Photopatterned collagen–hyaluronic acid interpenetrating polymer network hydrogels, Acta Biomater. 5 (7) (2009) 2385–2397.

[15] C. Mercado, J. Welling, M. Olivaq, J. Li, R. Gurung, S. Ruit, G. Tabin, D. Chang, D. Myung, Clinical application of a smartphone-based ophthalmic camera adapter in under-resourced settings in Nepal, J. Mobile Technol. Med. 6 (3) (2017) 34–42.

[16] C.M. Madl, L.M. Katz, S.C. Heilshorn, Bio-orthogonally crosslinked, engineered protein hydrogels with tunable mechanics and biochemistry for cell encapsulation, Adv. Funct. Mater. 26 (21) (2016) 3612–3620.

[17] B. Depalle, Z. Qin, S.J. Shefelbine, M.J. Buehler, Influence of cross-link structure, density and mechanical properties in the mesoscale deformation mechanisms of collagen fibrils, J. Mech. Behav. Biomed.l Mater. 52 (2015) 1–13.

[18] D. Palanker, Optical Properties of the Eye, AAO One Network, 2013.

[19] H. Wang, L. Cai, A. Paul, A. Enejder, S.C. Heilshorn, Hybrid elastin-like polypeptide–polyethylene glycol (ELP-PEG) hydrogels with improved transparency and independent control of matrix mechanics and cell ligand density, Biomacromolecules 15 (9) (2014) 3421–3428.

[20] L. Wang, A.M. Mahmoud, B.L. Anderson, D.D. Koch, C.J. Roberts, Total corneal power estimation: ray tracing method versus Gaussian optics formula, Invest. Ophthalmol. Vis. Sci. 52 (3) (2011) 1716–1722.

[21] T. Olsen, On the calculation of power from curvature of the cornea, Br. J. Ophthalmol. 70 (2) (1986) 152–154.

[22] M. Yazdani, A. Shahdadfar, C.J. Jackson, T.P. Utheim, Hyaluronan-based hydrogel scaffolds for limbal stem cell transplantation: a review, Cells 8 (3) (2019).

[23] H.J. Lee, G.M. Fernandes-Cunha, I. Putra, W.-G. Koh, D. Myung, Tethering growth factors to collagen surfaces using copper-free click chemistry: surface characterization and in vitro biological response, ACS Appl. Mater. Interfaces 9 (28) (2017) 23389–23399.

[24] M. Barile, D. Valenti, G.A. Hobbs, M.F. Abruzzese, S.A. Keilbaugh, S. Passarella, E. Quagliariello, M.V. Simpson, Mechanisms of toxicity of 3′-azido-3′-deoxythymidine: its interaction with adenylate kinase, Biochem. Pharmacol. 48 (7) (1994) 1405–1412.

[25] T. Nishimura, S. Toda, T. Mitsumoto, S. Oono, H. Sugihara, Effects of hepatocyte growth factor, transforming growth factor-β1 and epidermal growth factor on bovine corneal epithelial cells under epithelial–keratocyte interaction in reconstruction culture, Exp. Eye Res. 66 (1) (1998) 105–116.

[26] C.A. Gauthier, B.A. Holden, D. Epstein, B. Tengroth, P. Fagerholm, H. Hamberg-Nystrom, Role of epithelial hyperplasia in regression following photorefractive keratectomy, Br. J. Ophthalmol. 80 (6) (1996) 545–548.

[27] J. Chen, Z. Li, L. Zhang, S. Ou, Y. Wang, X. He, D. Zou, C. Jia, Q. Hu, S. Yang, X. Li, J. Li, J. Wang, H. Sun, Y. Chen, Y.T. Zhu, S.C.G. Tseng, Z. Liu, W. Li, Descemet's membrane supports corneal endothelial cell regeneration in rabbits, Sci. Rep. 7 (1) (2017) 6983.

[28] S.P. Sugrue, J.D. Zieske, ZO1 in corneal epithelium: association to the zonula occludens and adherens junctions, Exp. Eye Res. 64 (1) (1997) 11–20.